

Influence of CaCuO_2 Particle Size on Phase Evolution of Bi-based High Temperature Superconductors Prepared by Two-powders Route

Zhang Shengnan¹, Huang Yingjian², Ma Xiaobo¹, Cui Lijun³, Liu Guoqing¹,
Zheng Huiling¹, Xu Xiaoyan¹, Jiao Gaofeng¹, Li Chengshan¹, Feng Jianqing¹,
Yan Guo³, Zhang Pingxiang^{1,3}

¹ Northwest Institute for Nonferrous Metal Research, Xi'an 710016, China; ² Xi'an University of Technology, Xi'an 710048, China; ³ Western Superconducting Technologies Co., Ltd, Xi'an 710018, China

Abstract: $\text{Bi}_{1.76}\text{Pb}_{0.34}\text{Sr}_{1.93}\text{Ca}_{2.0}\text{Cu}_{3.06}\text{O}_{8+\delta}$ (Bi-2223) precursor powders were fabricated with a two-powder route based on co-precipitation process. During this process, $\text{Bi}_{1.76}\text{Pb}_{0.34}\text{Sr}_{1.93}\text{CaCu}_{2.06}\text{O}_{8+\delta}$ (Bi-2212) and CaCuO_2 (with the actual phase composition of Ca_2CuO_3 and CuO) powders were first synthesized and calcined separately, and then mixed together before packed into Ag sheath. By adjusting the pH values during the co-precipitation process, CaCuO_2 powders with different average particle sizes of about 1.10, 0.75, and 0.60 μm were obtained. Then single filament Bi-2223/Ag tapes were fabricated by powder in tube (PIT) process with precursor powders obtained by mixing the different particle sized CaCuO_2 powders and well-calcinated Bi-2212 powders. The influences of CaCuO_2 particle size on microstructure, phase evolution dynamics and superconducting current capacity of sintered Bi-2223 tapes were studied. Results show that due to higher uniformity of Ca_2CuO_3 and CuO distribution in filaments, clustering of secondary phases and insufficiently reacted areas are effectively avoided. Therefore, higher current density of $\sim 12\ 200\ \text{A}\cdot\text{cm}^{-2}$ is obtained for the 1# tape by further optimizing the final dimension of the tapes.

Key words: high temperature superconductor; Bi-2212; precursor powder; phase evolution dynamic; microstructure

Due to the high current capacity at liquid nitrogen temperature, $\text{Bi}_2\text{Sr}_2\text{Ca}_2\text{Cu}_3\text{O}_{10+\delta}$ (Bi-2223) is considered to be one of the most promising high temperature superconductors (HTS) for practical applications since its discovery in 1986^[1]. After several decades of research, the fabrication technique of Bi-2223, namely powder-in-tube process combined with a commercialized controlled over-pressure heat treatment process, has been well-developed^[2-5]. And the maximum critical current of $>270\ \text{A}$ at 77 K under self-field was reported by Sumitomo Electric Industries, Ltd. Furthermore, many demonstrative projects have been designed and carried out with Bi-2223 tapes, such as cables^[6, 7] and motors^[8, 9]. Recently, the

motors^[8, 9]. Recently, the possibility of fabricating high field magnets with Bi-2223 tapes has also been proved: Marshall et al^[10] achieves 5.5 T under 14 T background field in National High Magnetic Field Lab using the Bi-2223 coil, and Yanagisawa et al^[11, 12] from RIKEN achieves 4.5 and 6.5 T in sequence in 11 T background field using the Bi-2223 and REBCO coil.

Precursor powders with high Bi-2212 phase content, proper phase assemblage, as well as suitable particle size, are the most crucial factors for the fabrication of Bi-2223 tapes with high current capacity. Many methods have been proposed for the fabrication of Bi-2223 precursor powders,

Received date: May 10, 2019

Foundation item: National Natural Science Foundation of China (51472206); National ITER Program of China (2013GB110001); National Key Research and Development Program of China (2017YFB0902303)

Corresponding author: Zhang Shengnan, Ph. D., Senior Engineer, Superconducting Materials Research Center, Northwest Institute for Nonferrous Metal Research, Xi'an 710016, P. R. China, Tel: 0086-29-86231079, E-mail: snzhang@c-nin.com

Copyright © 2020, Northwest Institute for Nonferrous Metal Research. Published by Science Press. All rights reserved.

including high energy ball milling^[13], spray drying^[14, 15], spray pyrolysis^[16, 17], and co-precipitation process. Among these methods, co-precipitation process exhibits many advantages, such as low equipment requirement, high controllability and reliability. Therefore, many industrial companies fabricate Bi-2223 and Bi-2212 precursor powders using this method^[18, 19]. Based on previous studies, the appearance of both Bi_{1.76}Pb_{0.34}Sr₂CuO_{8+δ} (Bi-2201)^[20], due to the insufficient calcination of powders, or Bi-2223, due to the over-sintering of powders, should be avoided. However, considering the narrow formation window of Bi-2212 phase, it is very difficult to control the calcination process of precursor powders to avoid the formation of Bi-2201 and Bi-2223^[21, 22].

In previous work^[23-26], two-powder route based on co-precipitation technique was adopted, and (Bi, Pb)-2212 powders and CaCuO₂ which actually consists of Ca₂CuO₃ and CuO (1:1 molar ratio) were synthesized and calcined separately. The formation of a large content of properly sintered Bi-2212 phases is guaranteed. While during this process, the microstructure of CaCuO₂ should be very important for the phase evolution process, and the current capacity of final tapes. Thus, in this study, CaCuO₂ powders with different particle sizes were synthesized by tuning the pH values during co-precipitation process. The influences of CaCuO₂ particle size on the phase evolution dynamics, microstructures, as well as critical current density were systematically investigated.

1 Experiment

(Bi, Pb)-2212 precursor powders with the chemical composition of Bi_{1.76}Pb_{0.34}Sr_{1.93}CaCu_{2.06}O_{8+δ} were synthesized by co-precipitation process with the starting materials of Bi₂O₃, PbO, SrCO₃, CaCO₃ and CuO (>99.9%) as described in our previous study^[27]. CaCuO₂ powders with the actual phase composition of Ca₂CuO₃ and CuO were also synthesized by similar co-precipitation process. By tuning the pH values to 3.0, 5.0 and 6.5, CaCuO₂ powders with obviously different particle sizes were obtained, namely 1#, 2#, and 3# samples, respectively. After a series of calcination process combined with intermediate grinding, both powders with a main phase of Bi-2212 and Ca₂CuO₃+CuO were obtained separately. By mixing these two powders uniformly in a molar ratio of 1:1, precursor powders of Bi-2223 with a nominal composition of Bi_{1.76}Pb_{0.34}Sr_{1.93}Ca₂Cu_{3.06}O_{8+δ} were obtained. And a calcination process was performed under ambient atmosphere at 800 °C/3 h for carbon removal. Single filament Bi-2223/Ag tapes were fabricated by the typical powder in tube (PIT) technique. In order to investigate the influences of filament size, tapes with different final thicknesses of 0.35, 0.27, 0.23 and 0.20 mm were fabricated from different starting diameters of 1.86, 1.51

1.23 and 1.00 mm. Then a three-step sintering process was performed for the sintering of the as-rolled tapes with a length of 10 cm under the atmosphere of 7.5% O₂, during which the first heat treatment process (HT1) was performed at 824 °C for 15 h, the second heat treatment process (HT2) was at 824 °C for 50 h, and the post annealing process (PA) was at 780 °C for 20 h. An intermediate rolling was adopted between HT1 and HT2 for the further formation of Bi-2223 phase.

Polycrystalline X-ray diffraction (XRD) patterns of both precursor powders and sintered tapes were obtained by X-ray diffraction (XRD, Bruker D8 Advance) with Cu-Kα radiation. Microstructures of both precursor powders and tapes during different sintering processes were examined by scanning electron microscope (SEM) under secondary electron image (SEI) mode and backscattering electron image (BEI) mode. The compositional analysis was conducted by Inca-X-Stream energy-dispersive X-ray spectroscopy (EDX) to recognize the phase distribution. The phase distribution in BSI images was analyzed by a software named ImageJ®. The chemical composition of obtained precursor powders with the nominal chemical composition of Bi-2223 was determined by inductive coupled plasma atomic emission spectrometry (ICP-AES) with IRIS® Advantage ICP-AES. Transport critical current (*I_c*) was measured using standard DC four-probe method at 77 K and 0 T with the criterion of 1 μV/cm. Critical current density *J_c* was calculated as *J_c*=*I_c*/*A*, where *A* is the cross section of superconducting core.

2 Results and Discussion

XRD patterns of fully calcinated CaCuO₂ powders are obtained, as plotted in Fig.1a. The phase composition of these three powders is identical, all composed of Ca₂CuO₃ and CuO phases as designed. No detectable secondary phase can be observed in these three powders. However, with the increase of pH values during co-precipitation process, obvious increase of full-width at half-maximum (FWHM) is observed, as shown in the inset in Fig.1a. By refining the obtained patterns, FWHM values of (001) peak of Ca₂CuO₃ and (111) peak of CuO are estimated and plotted in Fig.1b. The FWHM values increase from 0.163° and 0.199° to 0.387° and 0.573° at different pH values, as listed in Table 1, representing the decrease of particle size of both Ca₂CuO₃ and CuO. Specific BET surface area measurement is also performed for different powders. As listed in Table 1, the average particle sizes are analyzed to be about 1100, 750 and 600 nm.

The SEM images of CaCuO₂ powders obtained at different pH values are shown in Fig.2a. In each image, there are basically two different particles, which are identified by EDX. The bigger ones with clean surface and polyhedron shapes can be recognized as Ca₂CuO₃ particles. The other smaller ones

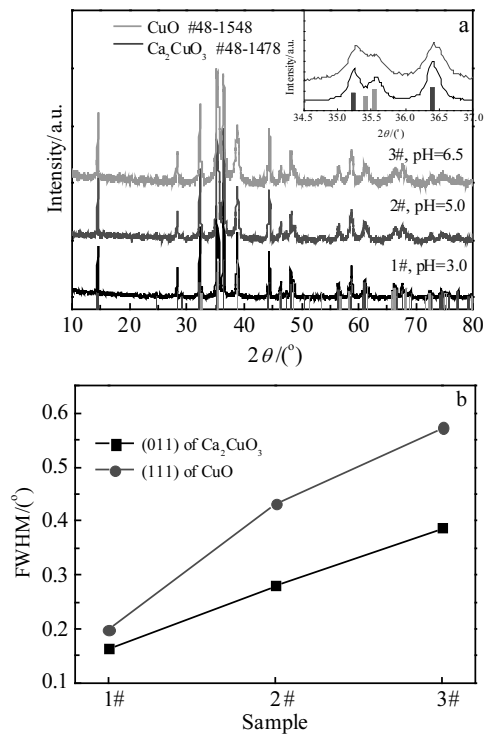


Fig.1 XRD patterns (a) of CaCuO_2 powders obtained at different pH values (certain peaks of both phases are zoomed in inset to show the broadening of peaks); FWHM of characterization peaks (b)

with spherical shape are regarded as CuO particles. The difference in particle size can be clearly observed in both low and high magnification images, as shown in insets. Both the difference in particle size between Ca_2CuO_3 and CuO, and its change with pH values are consistent with the analysis of XRD, which proves the effectiveness of controlling CaCuO_2 particle size by altering pH values.

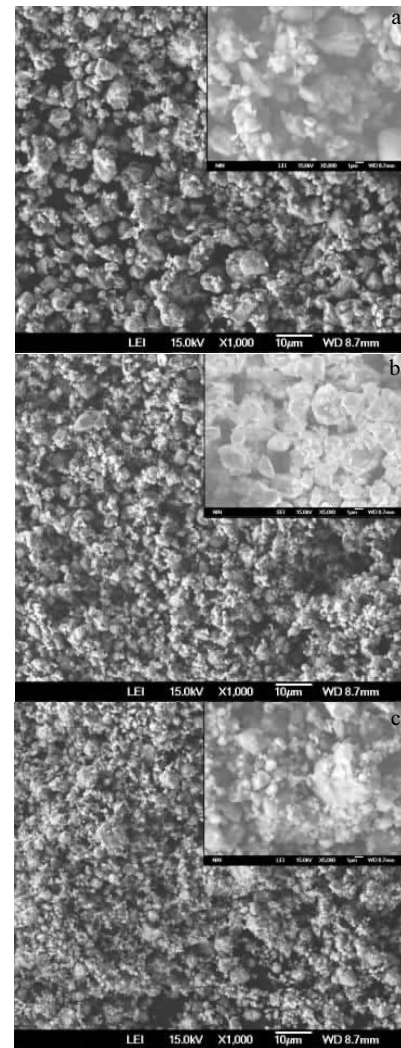


Fig.2 SEM images of CaCuO_2 powders at different pH values: (a) 1#, pH=3.0; (b) 2#, pH=5.0; (c) 3#, pH=6.5

Table 1 Physical parameters of CaCuO_2 and Bi-2223 precursor powders and related tapes

Parameter	1#	2#	3#
pH value	3.0	5.0	6.5
FWHM of (011) peak for Ca_2CuO_3 (°)	0.163	0.280	0.387
FWHM of (011) peak for CuO(°)	0.199	0.431	0.573
Particle size based on BET measurement/nm	1100	750	600
Bi content in Bi-2223 powders/wt%	34.31	34.60	34.28
Pb content in Bi-2223 powders/wt%	6.41	6.48	6.40
Ca content in Bi-2223 powders/wt%	7.33	7.41	7.35
Sr content in Bi-2223 powders/wt%	15.63	15.55	15.61
Cu content in Bi-2223 powders/wt%	18.42	18.45	18.34
Surface ratio of Bi-2223 after HT1/%	91.66	87.52	82.88
Surface ratio of Bi-2223 after PA/%	94.25	91.57	87.76
Maximum critical current density/ $\text{A}\cdot\text{cm}^{-2}$	12 205.94	9524.65	9351.44

In order to fabricate Bi-2223 tapes, CaCuO_2 precursor powders with different particle sizes are mixed with their corresponding completing component, Bi-2212, under the same planetary ball milling process. The chemical composition of these powders is characterized with ICP. As listed in Table 1, due to the small influences of pH values on the chemical composition of CaCuO_2 rather than Bi-2212 phase, the chemical composition variation of different powders are all within the error range of 1.0%. Therefore, the influences of chemical composition difference on the current capacity of final tapes can be ruled out.

After the mixture is packed into Ag tubes and standard drawing, swaging and rolling process, the green tapes are obtained. The cross section SEM images are obtained after polishing. The contrast in BSI should be attributed to the chemical composition variation of different phases. Therefore, the distribution of both Ca_2CuO_3 and CuO can be observed. As shown in Fig.3, based on EDX characterization, black particles are Ca_2CuO_3 phase and gray particles are CuO phase, which are slightly smaller than black particles. The distribution of Ca_2CuO_3 and CuO is mostly homogenous in Fig.3a. While, more and more clusters of Ca_2CuO_3 and CuO can be observed with the decrease of particle size. Both the increase of cluster number and clusters size is observed in the powders obtained at pH=6.5. The formation of clusters should be directly related to the larger specific surface areas and higher surface energy of small particles, which will deteriorate the homogeneity of Bi-2223 precursor components during phase evolution and consequently decrease the phase content of Bi-2223, texture alignment, and supposedly its electrical performance. Moreover, the formed clusters will also greatly obstacle the movement of powders during drawing process, thus leading to the formation of more cracks, which can also influence the current capacity of final tapes.

Single filament tapes are adopted for the phase evolution study. After sintering with HT1 process, the cross section of tapes is polished and SEM images are shown in Fig.4a~4c. Combining EDX analysis and the contrast of these BEI images, it can be deduced that after HT1 process, a large content of Bi-2223 phases form as the major phases. While

there are still considerable contents of secondary phases, including alkali earth cuprate ($(\text{Ca}, \text{Sr})_x\text{Cu}_y\text{O}_z$, AEC) phase and CuO. By analyzing these images with ImageJ, the area ratios of different phases, namely AEC+CuO+pores, which are mainly the dark particles, and Bi-2212 phase, which are light gray sheets, are obtained, as shown in Fig.4d. Obvious increase of secondary phase content with decrease of particle size can be clearly observed. Most secondary phases can be considered as the residual of Bi-2223 formation reactions, which is due to the insufficient reaction between Bi-2212 and original Ca_2CuO_3 and CuO. Therefore, it is the lack of Bi-2212 phase in cluster regions that should be attributed to the massive remaining of both AEC and CuO phases. It implies that the inhomogeneous distribution due to the formation clusters seriously delays the formation of Bi-2223 phase.

The SEM images of single filament tapes after PA process are obtained, as shown in Fig.5a~5c, and the surface ratios of secondary phases, namely AEC+CuO+ Pores, shown as dark particles, and Bi-2212+Pb-rich phase, shown as light particles, are obtained and shown in Fig.5d. After the PA process, a certain amount of Pb-rich phases, especially $\text{Pb}_3\text{Sr}_3\text{Ca}_2\text{CuO}_{12}$ (3321) phase, appear as light gray particles and are precipitated during the PA process, according to the previous studies^[28], which is responsible for the enhancement of intergrain connections. Obvious decrease of secondary phase content can be observed compared to the tapes after HT1. The phase content of CuO is larger than that of AEC phase. The particle size of CuO increases from 1# to 3# tapes, which is contrary to the original particle size results, implying that most CuO particles are newly formed during the sintering process. Therefore, the final particle size has nothing to do with original particles, but is related with the reaction equilibrium between different phases instead. Clusters, smaller than original ones, are still visible in 2# and 3# tapes, which still can be regarded as the residual of insufficient Bi-2223 formation reactions. The clusters, mainly composed of AEC phase, can be used to explain the increase content of CuO in Bi-2223 matrix. Meanwhile, it should be noticed that the characterization size of clusters of

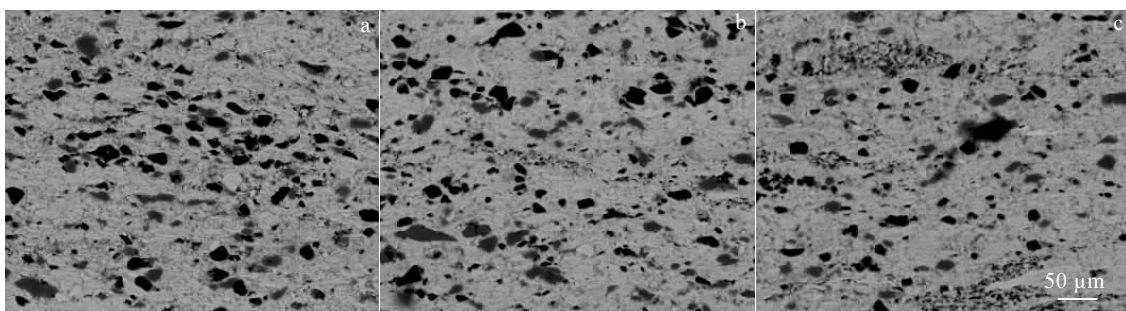


Fig.3 SEM images of green tapes packed with Bi-2212 and CaCuO_2 powders at different pH values: (a) 1#, pH=3.0; (b) 2#, pH=5.0; (c) 3#, pH=6.5

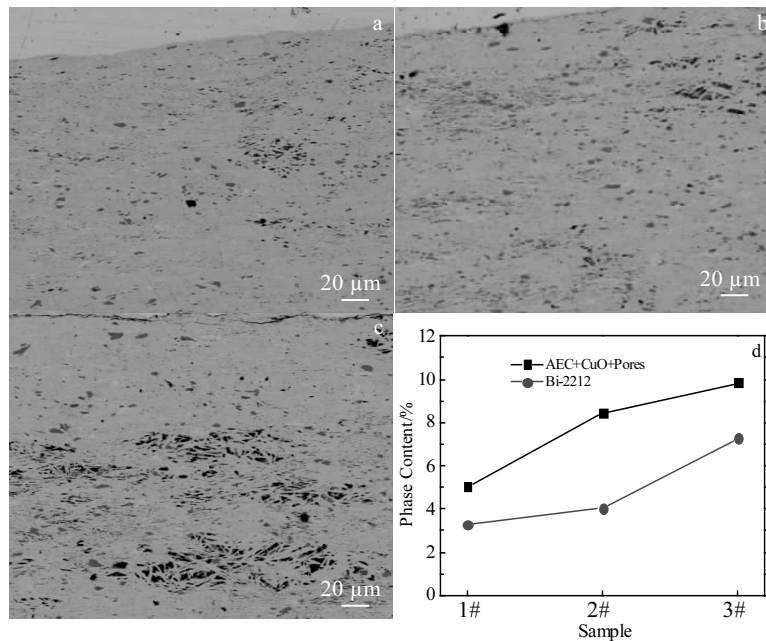


Fig.4 SEM images of sintered tapes after HT1 process packed with Bi-2212 and CaCuO_2 powders at different pH values: (a) 1#, pH=3.0; (b) 2#, pH=5.0; (c) 3#, pH=6.5; surface ratio of different phases (d)

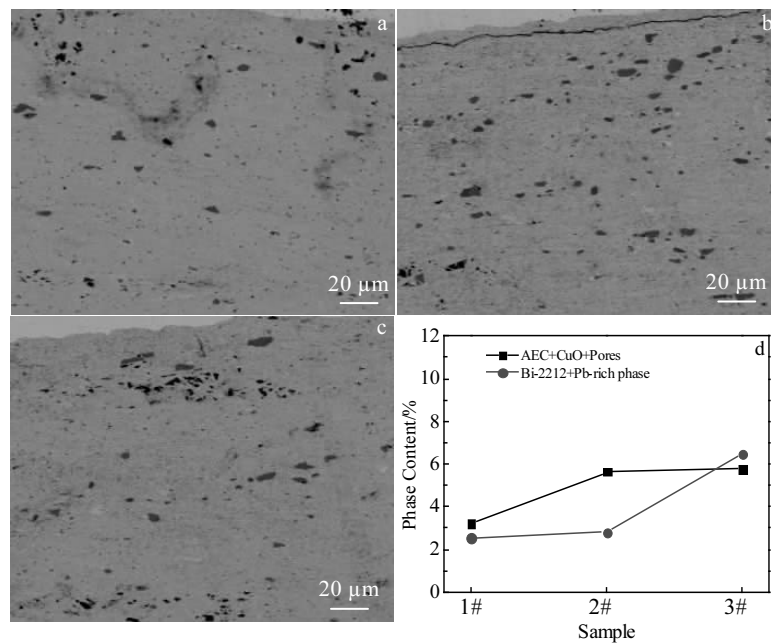


Fig.5 SEM images of sintered tapes after PA process packed with Bi-2212 and CaCuO_2 powders at different pH values: (a) 1#, pH=3.0; (b) 2#, pH=5.0; (c) 3#, pH=6.5; surface ratio of different phases (d)

20~40 μm is much larger than that of CuO (3~8 μm), so the influences of these clusters on both the textural structure of Bi-2223 grains and the current capacity of obtained tapes should be crucial.

The critical current density, I_c , of these single filament tapes after complete heat treatment process are obtained and listed in Table 1. The thickness of 0.35 mm combined

with the width of 4.6 mm is a typical structure for this procedure. However, as shown in Fig.1, the critical current density values of 0.35 mm thick tapes are very low, within the range of 3500~6500 $\text{A}\cdot\text{cm}^{-2}$. Therefore, we assume that it is the low filament density that should be accused for the weak intergrain connections, leading to low current capacity. In order to further enhance the intergrain connections,

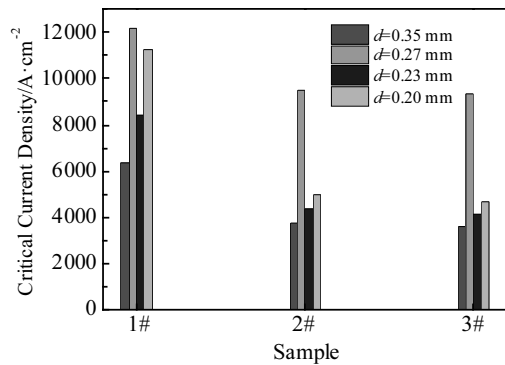


Fig.6 Critical current density of tapes with different thicknesses after complete heat treatment process

thinner tapes are obtained by applying large reduction rate of rolling process. Therefore, tapes with the cross section of $0.27\text{ mm}\times 3.4\text{ mm}$, $0.24\text{ mm}\times 3.0\text{ mm}$ and $0.20\text{ mm}\times 2.3\text{ mm}$ are obtained. As shown in Fig.6, the reduction of thickness is effective for the improvement of current capacity, which is more obvious for the 2# and 3# tapes. It can be explained that the reduction of tape thickness should contribute to both the enhancement of filament density and effective crush of some clusters. For 1# tape, the filament density enhancement mainly contributes to the J_c enhancement. As for 2# and 3# tapes, the effective crush of clusters leads to a more sufficient Bi-2223 formation reaction and less residual clusters, which also contributes to the J_c improvement. However, with the further decrease of tape thickness, more cracks can be formed and the current capacity exhibits a decreasing tendency again. Therefore, it can be concluded that the proper CaCuO_2 particle size for two-powder process should not be smaller than 750 nm and proper tape filament is also crucial for the final current capacity of tapes.

3 Conclusions

1) Both the grain size and particle size of CaCuO_2 can be controlled by tuning the pH values during co-precipitation process.

2) The decrease of CaCuO_2 particle size passing a threshold value can lead to the formation of considerable amounts of clusters in Bi-2223 green tapes, thus obviously affecting the Bi-2223 formation reaction.

3) The residual clusters can be crashed by decreasing the tape thickness. However, it is still the tape with the largest CaCuO_2 particle size that exhibits the maximum critical current density of over $12\ 200\ \text{A}\cdot\text{cm}^{-2}$.

References

1 Maeda H, Tanaka Y, Fukutomi M et al. *Japanes Journal of Applied Physics*[J], 1988, 27: 209

2 Masur L, Parker D, Tanner M et al. *IEEE Transactions on Applied Superconductivity*[J], 2001, 11(1): 3256

3 Malozemoff A P, Verebelyi D T, Fleshler S et al. *Physica C*[J], 2003, 386: 424

4 Yamade S, Ayai N, Fujikami J et al. *Physica C*[J], 2007, 463-465: 821

5 Hayashi K, Hikata T, Kaneko T et al. *IEEE Transactions on Applied Superconductivity*[J], 2001, 11(1): 3281

6 Xiao L Y, Dai S T, Lin L Z et al. *IEEE Transactions on Applied Superconductivity*[J], 2012, 22(3): 5 800 404

7 Ohmatsu K, Fujikami J, Taneda T et al. *Advances in Superconductivity XI* [M]. Tokyo: Springer, 1999: 817

8 Liu B, Badcock R, Shu H et al. *IEEE Transactions on Applied Superconductivity*[J], 2018, 28(4): 5 202 405

9 Gonzalez-Parada A, Espinosa-Loza F J, Castaneda-Miranda et al. *IEEE Transactions on Applied Superconductivity*[J], 2012, 22(3): 5 201 004

10 Marshall W S, Bird M D, Godeke A et al. *IEEE Transactions on Applied Superconductivity*[J], 2017, 27(4): 4 300 905

11 Yanagisawa Y, Kajita K, Iguchi S et al. *IEEE/CSC & ESAS Superconductivity News Forum*[J], 2016, 10: 42

12 Yanagisawa Y, Xu Y, Iguchi S et al. *Superconductor Science and Technology*[J], 2015, 28(12): 125 005

13 Darsono N, Imaduddin A, Raju et al. *Journal of Superconductivity and Novel Magnetism*[J], 2015, 28(8): 2259

14 Bao R, Song X H, Chen S S et al. *IEEE Transactions on Applied Superconductivity*[J], 2013, 23(3): 6 400 704

15 Ko J W, Yoo J M, Kim Y K et al. *Cryogenics*[J], 2003, 4(10-11): 549

16 Marinkovic B A, Jardim P M, Rizzo F et al. *Material Chemistry and Physics*[J], 2005, 94(2-3): 233

17 Yoo J M, Kim S W, Ko J W et al. *Superconductor Science and Technology*[J], 2004, 17(9): 538

18 Rey J M, Allais A, Duchateau J L et al. *IEEE Transactions on Applied Superconductivity*[J], 2009, 19(3): 3088

19 Bruzek C E, Lallouet N, Flahaut E et al. *IOP Conference Series*[J], 2004, 182: 2260

20 Guilmeau E, Andrzejewski B, Desgardin G *Physica C*[J], 2002, 377(3): 304

21 Majewski P. *Advanced Materials*[J], 2004, 6(6): 460

22 Kulakov A B, Bdikin I K, Zver'kov S A et al. *Physica C*[J], 2002, 371(1): 45

23 Ma X, Hao Q, Liu G et al. *Materials Letters*[J], 2016, 162: 5

24 Li J Y, Zheng H L, Li J G et al. *Material Science Forum*[J], 2007, 546-549: 1967

25 Xiong X M, Yu Z M, Zheng H L et al. *Chinese Journal of Low Temperature Physics*[J], 2005, 27(S1): 807

26 Mao C B, Zhou L, Sun X Y et al. *Physica C*[J], 1997, 281(1): 35

27 Mao C B, Du Z H, Zhou L. *Science in China*[J], 1996, 39(2): 181

28 Qu T M, Zhao L, Wang X C et al. *Physica C*[J], 2007, 463-465: 833

CaCuO₂ 颗粒尺寸对双粉法制备 Bi 系高温超导带材性能的影响

张胜楠¹, 黄英健², 马小波¹, 崔利军³, 刘国庆¹, 郑会玲¹, 徐晓燕¹, 焦高峰¹, 李成山¹,
冯建情¹, 闫果³, 张平祥^{1,3}

(1. 西北有色金属研究院, 陕西 西安 710016)

(2. 西安理工大学, 陕西 西安 710048)

(3. 西部超导材料有限公司, 陕西 西安 710018)

摘要: 通过基于共沉淀工艺的双粉法制备了 Bi_{1.76}Pb_{0.34}Sr_{1.93}Ca_{2.0}Cu_{3.06}O_{8+δ} (Bi-2223) 前驱体粉末。在这一过程中, 首先单独制备了 Bi_{1.76}Pb_{0.34}Sr_{1.93}CaCu_{2.06}O_{8+δ} (Bi-2212) 和 CaCuO₂ (实际相组成为 Ca₂CuO₃ 和 CuO) 粉末, 并分别进行了烧结。通过调节共沉淀工艺过程中的 pH 值, 获得了颗粒尺寸不同的 CaCuO₂ 粉末, 然后将 Bi-2212 与 CaCuO₂ 粉末按照相组成 1:1 进行混合, 并装入 Ag 包套中, 通过一系列的旋锻、拉拔和轧制工艺, 获得设计尺寸的 Bi-2223 带材。比表面积测试表明随着 pH 值从 3.0 增加到 5.0 和 6.5, 获得 CaCuO₂ 粉末的平均颗粒尺寸从 1.10 μm 减小到 0.75 和 0.60 μm。通过扫描电镜对不同尺寸 CaCuO₂ 颗粒制备的 Bi-2223 生带、第 1 次热处理和后处理之后带材的相组成和分布进行了表征。结果表明, 适当尺寸的 CaCuO₂ 颗粒可以避免团聚现象的出现, 因此有利于高载流性能带材的获得。最终通过进一步调节带材的尺寸, 1#带材的性能最高, 电流密度达到了约 12 200 A·cm⁻²。

关键词: 高温超导材料; Bi-2212; 前驱体粉末; 相演变动力学; 微结构

作者简介: 张胜楠, 女, 1983 年生, 博士, 高级工程师, 西北有色金属研究院超导材料研究所, 陕西 西安 710016, 电话: 029-86231079, E-mail: snzhang@c-nin.com